Published by IOP Publishing for Sissa Medialab

Received: *December 8, 2023*
Revised: *February 9, 2024*
Accepted: *February 12, 2024*
Published: *April 2, 2024*

16th Topical Seminar on Innovative Particle and Radiation Detectors
Siena, Italy
25–29 September 2023

Characterization of the FOOT neutron detectors for nuclear fragmentation measurements at the n_TOF facility

R. Zarrella[a,b,*] **A. Manna**[a,b] **S. Amaducci**[c] **M. Bacak**[d] **A. Casanovas**[e] **S. Colombi**[b] **C. D'Orazio**[a,b] **F. García-Infantes**[f,d] **N. Malekinezhad**[g,a] **M. Marafini**[h,i] **C. Massimi**[a,b] **A. Mengoni**[j,b] **A. Musumarra**[k,l] **N. Patronis**[m,d] **J.A. Pavón-Rodríguez**[f,d] **M.G. Pellegriti**[l] **R. Spighi**[b] **E. Stamati**[m,d] **and M. Villa**[a,b] **on behalf of the FOOT and n_TOF collaborations**

[a] *Department of Physics and Astronomy, University of Bologna, Bologna, Italy*
[b] *INFN Section of Bologna, Bologna, Italy*
[c] *INFN Laboratori Nazionali del Sud, Catania, Italy*
[d] *European Organization for Nuclear Research (CERN), Geneve, Switzerland*
[e] *Universitat Politècnica de Catalunya, Barcelona, Spain*
[f] *University of Granada, Granada, Spain*
[g] *Shahrood University of Technology, Shahrood, Iran*
[h] *INFN Section of Roma 1, Rome, Italy*
[i] *Museo Storico della Fisica e Centro Studi e Ricerche Enrico Fermi, Rome, Italy*
[j] *Agenzia nazionale per le nuove tecnologie (ENEA), Roma, Italy*
[k] *Department of Physics and Astronomy, University of Catania, Catania, Italy*
[l] *INFN, Section of Catania, Catania, Italy*
[m] *University of Ioannina, Ioannina, Greece*

E-mail: roberto.zarrella2@unibo.it

Abstract: FOOT (FragmentatiOn Of Target) is an applied nuclear physics experiment with the aim of performing high precision cross section measurements for fragmentation reactions of interest in hadrontherapy and radiation protection in space. The physics program of the experiment foresees a set of measurements with light ion beams, such as C and O, in the energy range of 100–800 MeV/u interacting with tissue-like and shielding material targets. The setup was initially conceived for the detection of charged fragments and, in 2021, the Collaboration started the study of possible solutions for neutron detection. Two detection systems have been proposed: one based on BC-501A liquid

*Corresponding author.

https://doi.org/10.1088/1748-0221/19/04/C04006

2024 JINST 19 C04006

scintillators with neutron/γ discrimination capabilities and a system based on BGO crystals operated in phoswich mode. In 2022, a dedicated data acquisition campaign was carried out at the n_TOF facility at CERN to evaluate the capabilities of the two systems. First, the neutron/γ discrimination efficiency of the BC-501A system was studied using radioactive sources. Then, the two systems were placed in the n_TOF experimental area to study their neutron detection efficiency under a well characterized neutron beam. In this work, the first preliminary results concerning the characterization of the two possible neutron detectors of FOOT are presented.

KEYWORDS: Neutron detectors (cold, thermal, fast neutrons); Scintillators, scintillation and light emission processes (solid, gas and liquid scintillators)

2024 JINST 19 C04006

Contents

1 Introduction

Hadrontherapy is a commonly used treatment modality for deep-seated solid tumors. The primary benefit of this technique is the more conformal dose distribution that can be achieved with proton and ion beams in comparison to X-rays, which significantly lowers the collateral damage to healthy tissues. However, the impact of nuclear fragments to dose profiles is yet to be accurately evaluated. In fact, cross section data for fragmentation reactions at therapeutic energies (up to 400 MeV/u) are scarce and restricted to a small number of projectiles and targets [1].

Nuclear fragmentation reactions are also important for radiation protection in space. Astronauts are constantly exposed to ionizing radiation from several sources while in space. In order to design novel shielding materials and accurately assess the radiation-induced health risks in long-term space missions, such as travel to Mars, a thorough understanding of how this radiation interacts with the various materials that make up spaceship hulls is essential [2].

In both research fields, most of the calculations are performed using Monte Carlo transport codes based on phenomenological models of nuclear interactions. However, the lack of experimental cross section data for nuclear fragmentation in the energy range between 100 and 800 MeV/u means that the description of such reactions is still subject to significant uncertainties. This makes it extremely difficult to estimate the contribution of secondary nuclear fragments to radiation exposure and damage. In particular, almost no information on secondary neutron production is available, introducing unavoidable uncertainties on the assessment of the associated radiation risk [3].

2 The FOOT experiment

The goal of the FOOT (FragmentatiOn Of Target) experiment is a full characterization of the nuclear fragmentation reactions of interest for hadrontherapy and radiation protection in space in the projectile energy range between 100 and 800 MeV/u. The final objective is the measurement of double differential fragmentation cross sections in both kinetic energy and diffusion angle. FOOT has been conceived to measure the kinematic characteristics of the produced nuclear fragments, allowing for precise particle identification. The apparatus, made of different types of detectors, has been developed to characterize both the primary beam and all the secondary fragments coming from nuclear reactions with the target in order to perform measurements in inverse kinematics and with composite targets [4].

2024 JINST 19 C04006

To carry out the FOOT physics program, the setup has been conceived to be portable in order to exploit the different particle beams available in different facilities (i.e. CNAO in Italy or GSI in Germany). Two complementary setups have been developed: one based on nuclear emulsion films, mainly dedicated to the characterization of fragments with $Z \leq 3$, and one made of electronic devices, focused on heavier fragments ($2 \leq Z \leq 8$). The Emulsion Spectrometer will not be discussed since it is not the subject of this work, but detailed information can be found in [5].

The Electronic Setup of FOOT, shown in figure 1, is configured as a fixed target experiment. The apparatus is divided in three sections: the upstream region, devoted to the characterization of primary particles impinging on the target, measures their passage time and direction; the magnetic spectrometer, which performs track reconstruction and measures the momentum of nuclear fragments produced in the target; the downstream region, mainly devoted to particle identification through Time-Of-Flight, energy loss and kinetic energy measurements [6].

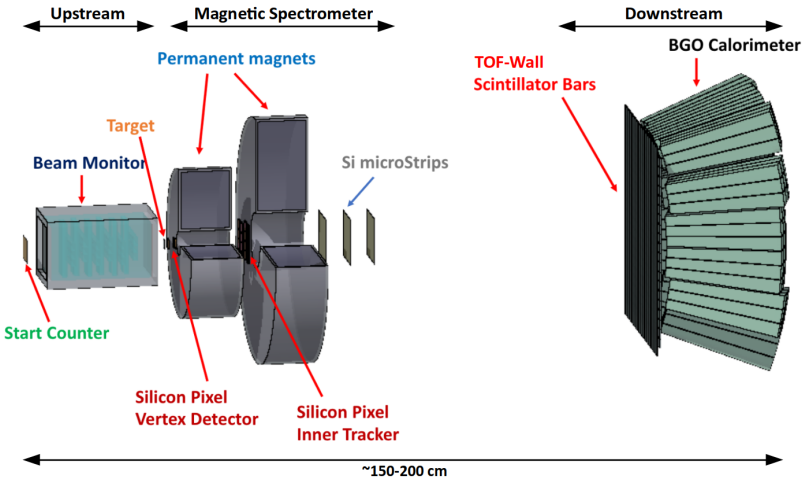

Figure 1. Sketch of the FOOT electronic setup obtained in the FLUKA framework. The three main regions of the apparatus are highlighted.

The setup has been conceived for the detection and characterization of charged fragments. However, one of the most complex and unsolved issues in hadrontherapy and radiation protection in space is the assessment of the neutron induced damage [7]. Contrary to charged particles, fast neutrons ($E \geq 10$ MeV) have a very long mean free path inside the human body, meaning that they can thermalize and consequently cause biological damage to tissues far from the point of production. In addition, the assessment of neutron-induced damage suffers from even higher uncertainties than for charged particles, since cross section data of neutron production are almost completely missing in the energy range between 100 and 800 MeV/u. To address this additional problem, in 2021, the FOOT collaboration started the development of dedicated neutron detectors.

3 The FOOT neutron detectors

Among the devices currently studied in FOOT as possible neutron detection upgrades, two systems are already available for use in experimental campaigns. The first system consists of a liquid scintillator (BC501-A), coupled with a PMT, sensitive to neutral particles, combined with an EJ200 plastic scintillator in front, readout using a SiPM, which acts as a veto for charged particles. The active

2024 JINST 19 C04006

volume of the detector has a cylindrical shape with 3 inches diameter and 3 inches height. The BC501-A has been chosen for its good time resolution and its different light response to neutrons and γ-rays. The n-γ discrimination is a fundamental prerequisite. As a matter of fact, after removing charged particles through anti-coincidence with the veto, the main source of background for neutron detection is γ-rays. A picture of the detectors is reported in figure 2(a).

The second system consists of a Phoswich detector based on BGO crystals optically coupled with a 3 mm thick EJ232 plastic scintillators in front. A prototype of the device is shown in figure 2(b). The crystals have a truncated pyramid shape, with 2.4×2.4 cm^2 front area, 3.3×3.3 cm^2 rear area and 24 cm length. The BGO Phoswich is being developed as a possible upgrade of the current FOOT calorimeter, which is made of 333 BGO crystals [8]. The coupling with a fast plastic scintillator is meant to strongly improve the time response for charged particles, maintaining the slower rise time of the BGO on neutron signals, allowing for particle discrimination capability without a separate veto detector.

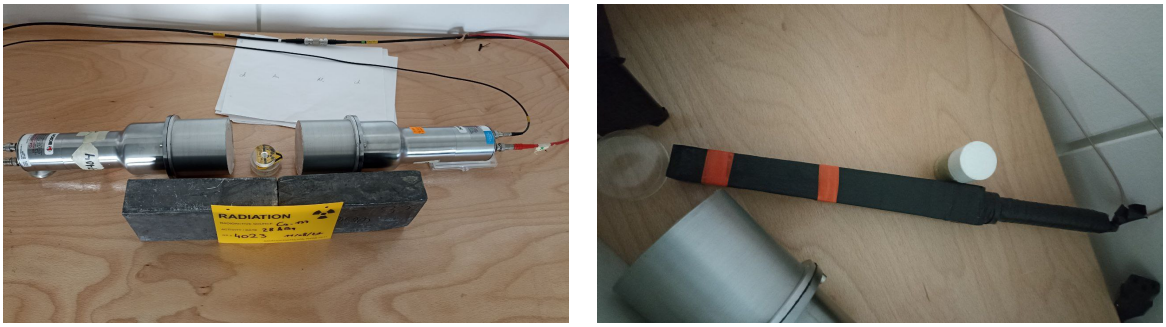

(a) (b)

Figure 2. FOOT neutron detector prototypes during tests with radioactive sources. (a) BC501-A liquid scintillators and (b) BGO crystal in phoswich mode.

However, before being available for experimental campaigns, both devices still require a precise evaluation of their neutron detection efficiency, which can only be obtained by irradiation under well-characterized neutron beams. For what concerns the BC-501A systems, another important feature to evaluate is their efficiency in terms of n-γ discrimination. Very few facilities in the world are capable of providing a neutron beam in the energy range explored by the FOOT physics program, i.e. 1–1000 MeV. To carry out the characterization campaign, the best option available was the n_TOF facility [9].

4 Detector characterization at the n_TOF facility

The neutron Time Of Flight (n_TOF) facility is a pulsed neutron source based at CERN. At n_TOF, the neutron beam is produced by spallation of the 20 GeV/c proton beam provided by the Proton Synchrotron (PS) impinging on a lead target. The neutrons generated in the target fly through the different beam lines of the facility, which lead to the three experimental areas:

- EAR1, placed at a distance of 185 m from the target. The neutron beam line is horizontal and tilted of 10° with respect to the direction of impinging protons.
- EAR2, placed at 20 m from the target, vertically at 90° with respect to the proton beam direction.
- NEAR, placed at only 3 m from the target, behind a shielding wall and a collimator.

2024 JINST 19 C04006

The PS proton bunches have an intensity of 3–8 $\times$ 10^{12} particles/bunch and the spallation reaction can yield up to 350 neutrons per incident proton, resulting in a very high instantaneous neutron flux in all the experimental areas [9].

The main characteristic of n_TOF is its capability of measuring the energy of the generated neutrons with an extremely good resolution, of the order of 10^{-3}–10^{-5}. This level of precision is achieved through the Time-Of-Flight technique. As a matter of fact, the spallation reaction, combined with borated-water moderation system, produces neutrons of energy ranging from thermal to GeV. These particles cover the flight paths to the experimental areas with very different TOF, which is directly related to the energy of the neutron at the time of production. Knowing the length of the flight path L, the kinetic energy E of the neutron can be calculated for TOF as

$$\begin{cases} E = mc^2(\gamma - 1) \\ \gamma = \sqrt{\left(1 - \frac{L^2}{c^2 \mathrm{TOF}^2}\right)^{-1}} \end{cases} \qquad \frac{\Delta E}{E} \underset{\sim}{\propto} \frac{\Delta v}{v} = \sqrt{\left(\frac{\Delta \mathrm{TOF}}{\mathrm{TOF}}\right)^2 + \left(\frac{\Delta L}{L}\right)^2} \tag{4.1}$$

In particular, the very long flight path of n_TOF EAR1 makes it very suitable for the characterization of the FOOT neutron detectors [10]. In order to comply with the dense physics program of the facility, the FOOT detectors were actually mounted in the Neutron Escape Line (NEL) of EAR1,with the aim of acquiring data downstream of the experimental area in a parasitic way.

In principle, in order to extract the neutron-detection efficiency of the two systems, it should be sufficient placing them directly on the neutron beam and measure the number of events detected. The comparison between this number and the known neutron flux in the experimental area provides the detection efficiency. However, this approach is really complicated to follow because of the so-called "γ-flash". This term indicates the first signal reaching the experimental area after a collision of the proton beam on the spallation target and it is generated by γ-rays and ultra-relativistic particles. This very intense pulse blinds the readout electronics of the detectors for a certain amount of time, posing a limit on the minimum TOF, and thus maximum neutron energy, detectable in the experimental area. In our case, the effect of the γ-flash has been mitigated by placing the detectors out of the beam line at a fixed angle and exploiting the neutron-proton elastic scattering on a H-rich target placed on beam. The final setup is sketched in figure 3. The sample was placed at a distance of about 200 m from the lead spallation target, perpendicular to the direction of incoming neutrons. The mechanical structure of the setup was made of aluminum frames with the possibility to slide and adjust the distance and angle of the detectors with respect to the target.

Thanks to the kinematics of the n-p elastic scattering reaction, the number of protons and neutrons produced via n-p elastic scattering and hitting the detectors is the same. The detection efficiency can be considered 100% for charged particles, therefore the ratio between the number of detected neutrons and protons gives a measurement of the neutron detection efficiency. An additional way to determine the neutron-detection efficiency is the comparison between the number of detected neutrons with the expected one, calculated from the evaluated neutron flux in the experimental area multiplied by the n-p elastic scattering differential cross section. This is possible because the n-p elastic scattering cross-section is very well known and it is considered the main reference for the high-energy-neutrons-induced reactions [11].

The discrimination of signals generated in the detectors by charged and neutral particles can be obtained requesting the coincidence and anti-coincidence between the events in the VETO (plastic

2024 JINST 19 C04006

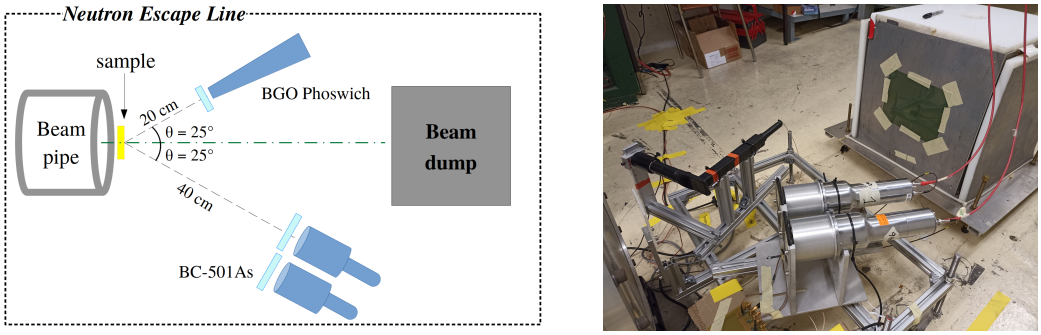

(a) (b)

Figure 3. Setup used for the data acquisition campaign in the NEL of n_TOF EAR1. (a) Schematic view of the apparatus, showing the distances and angles of the detectors with respect to the sample and (b) picture of the mounted experimental setup.

scintillator in front) and each device. The additional veto placed in front of the BGO crystal was used to verify the different phoswich responses to charged particles and neutrons. This information is crucial to assess the particle identification capabilities of the detector by itself, without the need for the veto.

The energy E_n of a neutron impinging on the detectors, after the elastic scattering in the sample, has to be calculated as

$$E_n = E'_n \cos^2(\theta) \tag{4.2}$$

where E'_n is the energy of the primary neutron undergoing the scattering, obtained from the TOF technique with equation (4.1), and θ is the scattering angle, i.e. the one fixed by the detectors position. From equation (4.2), it is clear that the energy resolution is dominated by the uncertainty on the scattering angle θ, which in turn depends on the geometry of the setup. The final distance of the detectors from the sample was chosen as a trade-off between a maximum uncertainty on the energy of detected neutrons of about 10–15%, while limiting the impact of the γ-flash and acquiring the highest statistics achievable.

During the measurement campaign, it was impossible to utilize a pure H target due to the need of keeping it at cryogenic temperatures. The solution was to perform the measurement with multiple samples. In particular, both polyethylene (PE, C_2H_4) and graphite targets of the same mass thickness were alternatively employed, using the latter to evaluate and subtract the background generated in the detectors by particles coming from n + C reactions. Moreover, since our detectors are also sensitive to γs, data were also acquired without any target on the neutron beam line to evaluate the background generated by the materials surrounding the setup. In such way, it is possible to select only the events generated from the interactions of the neutron beam with the hydrogen nuclei.

5 Preliminary results

For what concerns the BC-501A system, the first test carried out was an assessment of the n-γ discrimination capabilities. This was performed in laboratory by exposing the detector to different sources of either neutrons (^{252}Cf), γ rays (^{88}Y) or both (AmBe). Particle discrimination was achieved through Pulse Shape Analysis with the aim of decomposing the signal in a fast and a slow component. In fact, the

2024 JINST 19 C04006

different interaction of neutrons and gammas in the liquid scintillator results in a different light response and therefore in a different characteristic signal shape. In this case, the fast component was defined as the portion of the signal acquired within 10 ns of its onset, while the slow component was the rest of the signal tail. The two portions of the pulse were integrated separately, yielding results as those shown in figure 4(a), where data from an AmBe source are shown. The two visible populations are given by γ-rays and neutrons, with the latter recognizable in the lower portion of the graph where the slow component is dominant. Figure 4(b) shows the amplitude spectra of the signal obtained with the AmBe source and its neutron and γ components obtained through a selection performed using a parabolic cut in figure 4(a). As it can be seen, the Compton edge visible in the total spectrum is completely associated with the component given by γ-rays, indicating a good particle discrimination efficiency. A first study performed using the data acquired with the AmBe source has shown that it is possible to achieve an n-γ discrimination efficiency of around 90% with the current system. Data obtained with the other sources will be used to further asses the discrimination efficiency when only neutrons or γs impinge on the detectors.

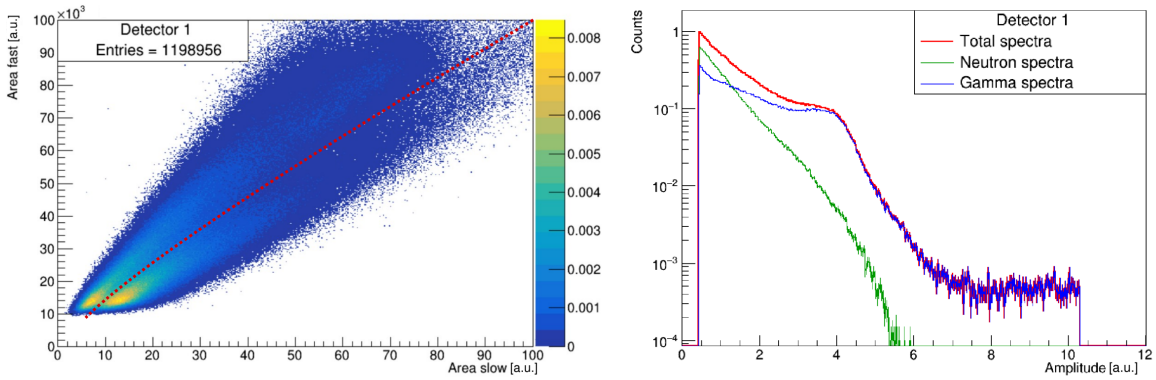

(a) (b)

Figure 4. Neutron-γ discrimination capabilities of the BC-501A detector with an AmBe source. (a) shows the relation between the area (integral) of the fast and slow components of signals, highlighting two populations. The dashed red line indicates the parabolic cut applied to separate neutrons and γ-rays. (b) Contribution of each population to the spectrum of the source.

After the characterization with radioactive sources, the detectors were mounted in the experimental area to acquire data with the neutron beam. Figure 5 shows the amplitude of registered signals as a function of TOF obtained for one of the BC-501A systems with the neutron beam impinging on a 2 mm PE sample. Here and in all the following plots, the TOF is reported taking the time of the γ-flash as reference, i.e. TOF = $t_{\text{signal}} - t_{\text{flash}}$. The actual TOF-energy conversion needs to take into account this component, which for a 200 m long flight path is $t_{\text{flash}} \simeq 667$ ns.

The time window chosen to define a coincidence event between a signal in the VETO and in the BC-501A was of ± 10 ns. It can be noticed that, except for a minor background given by random events, coincidence signals start only when the energy of the scattered particle is enough to punch through the plastic scintillator. The branch mainly visible in the events recorded in the VETO and defined in coincidence (figure 5(a)) is generated by charged particles coming from elastic n-p reactions. These events show the typical decreasing in the signal amplitude at higher neutron energies (lower TOF), which corresponds to higher energy of the charged particle entering the detector (i.e. lower deposited energy). The same structure can be observed also in figure 5(c) for anti-coincidences, with the addition

2024 JINST 19 C04006

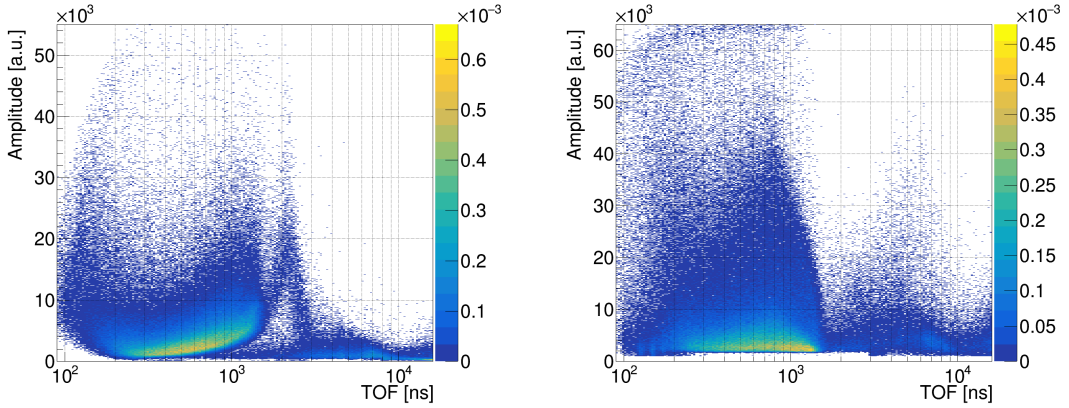

(a) VETO signals coincidence events

(b) BC-501A signals coincidence events

(c) VETO signals anti-coincidence events

(d) BC501A signals anti-coincidence events

Figure 5. Amplitude of the registered signals as a function of TOF for coincidence and anti-coincidence events for the BC501-A system. The reported counts are normalized to the number of PS proton pulses impinging on the n_TOF spallation target.

of the ascending branch, at higher TOF, coming from lower energy particles which reach the VETO but can not punch through it. The presence of signals above the punch-through energy threshold is due to the higher geometrical acceptance of the VETO with respect to the BC-501A detector.

Figure 5(b) shows a typical response of charged particles, for which the BC-501A works as a calorimeter until the impinging nuclei have enough energy to punch through the detector itself. Figure 5(d) shows the amplitude-TOF spectrum of the BC-501A for anti-coincidence events, i.e. neutral particles. The response of the detector is noticeably different in this case and much more complicated to understand. The high-amplitude signals at low TOF are generated by the tail of the γ-flash, which has a strong impact on the BC-501A due to its high angular acceptance. The influence of such signals for TOF < 200 ns, translates in the possibility to perform the characterization of this detectors up to about 550 MeV of impinging neutron energy. Moreover, the increase of counts at higher TOF values ($5–9 \cdot 10^3$ ns) is due to signals from γ-rays. These are, in fact, mainly produced in the interactions between the neutron beam and the Al window at the end of the beam pipe and their production probability is higher at lower neutron energies. The final interpretation of the results obtained with anti-coincidence events is currently ongoing. An in-depth understanding of the response

2024 JINST 19 C04006

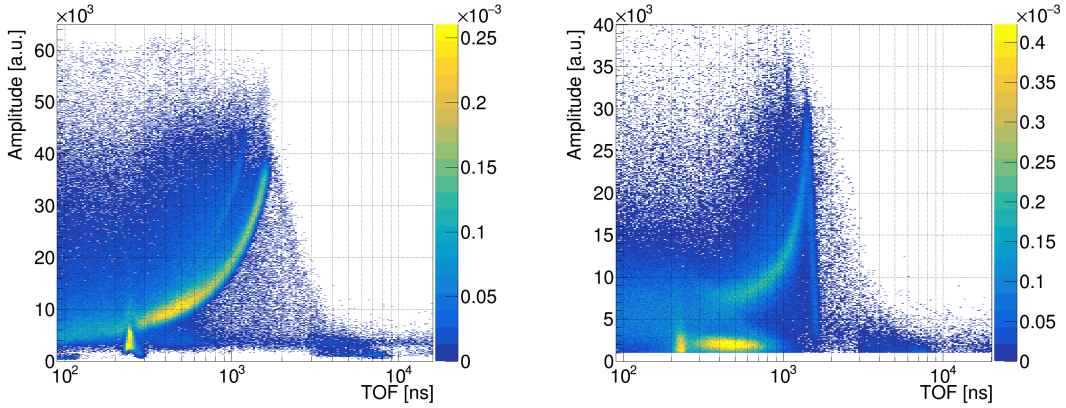

(a) VETO signals coincidence events

(b) BGO signals coincidence events

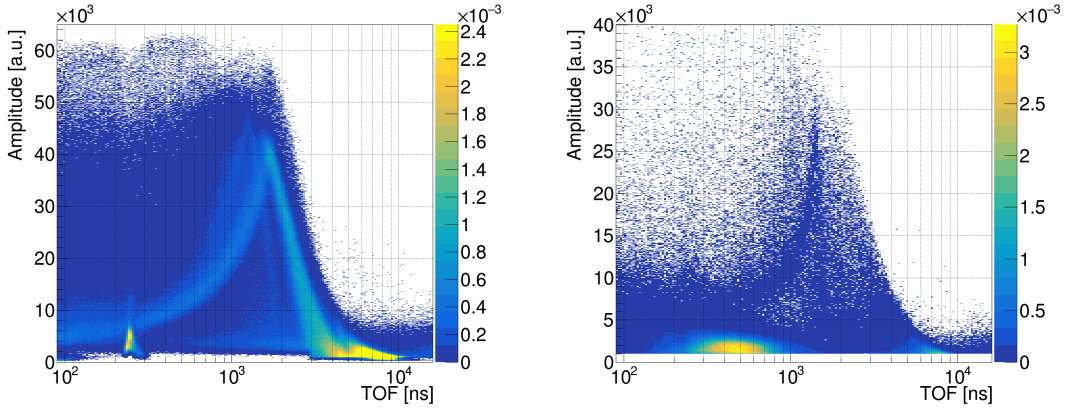

(c) VETO signals anti-coincidence events

(d) BGO signals anti-coincidence events

Figure 6. Amplitude of the registered signals as a function of TOF for coincidence and anti-coincidence events for the BGO phoswich system. The reported counts are normalized to the number of PS proton pulses impinging on the n_TOF spallation target.

to the neutron beam depends on the full characterization of n-γ discrimination capabilities and on a careful evaluation of the contribution coming from spurious coincidences and background events.

Figure 6 contains the same results addressed in figure 5 obtained for the VETO-phoswich BGO crystal combination. In this case, given the slightly worse time resolution of the phoswich system, the time coincidence window between VETO and BGO was fixed at ±12 ns. The graphs shown in figure 6(a) and 6(c) for the VETO can be understood with the same considerations made for the other detection system. The main difference is the thickness of the plastic scintillator, which is much larger in this case. This increases the punch-through energy and yields a better energy resolution. As a matter of fact this VETO, contrary to the one of the BC-501A system, is able to discriminate between signals produced by different charged particles. In the case of figure 6(a) and 6(c), the two visible branches are generated by protons and deuterons created in beam-target interactions. As for the BC-501A system, the VETO had a higher geometrical acceptance than the detector, which justifies the presence of anti-coincidence signals for charged particles above the punch-through energy. In figure 6(a) and 6(c) an excess of low-amplitude counts can be noticed at TOF $\simeq 2\text{–}3 \cdot 10^2$ ns. This effect is an artifact coming from an after-pulse in the PMT of the VETO detector that appears at a fixed time after the γ-flash. A way to completely remove these signals at the reconstruction level is currently being studied.

2024 JINST 19 C04006

Concerning the BGO detector, the request for coincidence signals yields the results shown in figure 6(b). Here, the two branches visible in the VETO are also distinguishable, meaning that the coincidence signals mostly come from the light generated in the plastic scintillator of the phoswich system. Thus, as expected, charged particle signals are dominated by the fast component of the BGO. On the contrary, the anti-coincidence signals (figure 6(d)) do not contain at all this component. Instead, there is a clear prevalence of higher energies events for which the slow component, characteristic of the BGO, is dominant. Moreover, the γ-ray background pointed out in figure 5(d), can be noticed also for the BGO detector in the same TOF range (5–9 $\cdot$ 10^3 ns). Further studies are needed to accurately evaluate the background generated by n+C reactions and by residual γ-rays, which can be assessed through the dedicated acquisitions without a target on the beam line. Nevertheless, the results reported in figure 6 indicate that the phoswich system, for charge particle discrimination, appears to work as expected. Hence, it can be asserted that the detector could constitute a viable upgrade of the current FOOT setup once its neutron detection capabilities are carefully determined.

6 Conclusions

A characterization campaign for the inclusion of neutron detectors in the FOOT experiment has been carried out at the n_TOF facility at CERN. Two possible detection systems have been studied as possible upgrade of the FOOT setup, one based on BC-501A liquid scintillators and the other one on BGO crystals operated in phoswich mode. The preliminary results, shown in this work, highlight that the first system has shown good particle discrimination capabilities, achieving an n-γ discrimination efficiency of about 90%. Moreover, the signal discrimination capabilities of the BGO phoswich system show that it can be effectively used to separate charged and neutral particles.

The results obtained with the neutron beam at the Neutron Escape Line of n_TOF experimental area 1 (EAR1) are currently being carefully studied. The coincidence analysis performed shows promising results for both detection systems, with the final evaluation of the neutron detection efficiency currently ongoing.

Acknowledgments

The FOOT Collaboration acknowledges the INFN sections of Bologna and Rome for the support in the preparation of the detectors and the mounting of the setup. The authors would like to thank the n_TOF Collaboration for the beam time granted at the facility to perform the measurement, as well as for the scientific and technical support provided throughout the whole experimental campaign.

References

[1] J.S. Loeffler and M. Durante, *Charged particle therapy-optimization, challenges and future directions*, *Nat. Rev. Clin. Oncol.* **10** (2013) 7.

[2] F.A. Cucinotta and M. Durante, *Cancer risk from exposure to galactic cosmic rays: implications for space exploration by human beings*, *Lancet Oncol.* **7** (2006) 431.

[3] F. Luoni et al., *Total nuclear reaction cross-section database for radiation protection in space and heavy-ion therapy applications*, *New J. Phys.* **23** (2021) 101201 [arXiv:2105.11981].

[4] FOOT collaboration, *FOOT Conceptual Design Report*, (2017), DOI:10.13140/RG.2.2.35295.30883.

2024 JINST 19 C04006

[5] G. Galati et al., *Charge identification of fragments with the emulsion spectrometer of the FOOT experiment*, *Open Phys.* **19** (2021) 32.

[6] G. Battistoni, M. Toppi and V. Patera, *Measuring the Impact of Nuclear Interaction in Particle Therapy and in Radio Protection in Space: the FOOT Experiment*, *Front. Phys.* **8** (2021) 568242.

[7] U. Schneider and H. Roger, *The Impact of Neutrons in Clinical Proton Therapy*, *Front. Onc.* **5** (2015) 235.

[8] L. Scavarda, *Design and performance of the Calorimeter for the FOOT experiment*, *Nuovo Cim. C* **43** (2020) 123.

[9] n_TOF collaboration, *The neutron Time-Of-Flight facility, n_TOF, at CERN (I): Technical Description*, TOF-PUB-2013-001 (2013).

[10] C. Guerrero et al., *Performance of the neutron time-of-flight facility n_TOF at CERN*, *Eur. Phys. J. A* **49** (2013) 27.

[11] A.D. Carlson et al., *International Evaluation of Neutron Cross Section Standards*, *Nucl. Data Sheets* **110** (2009) 3215.

2024 JINST 19 C04006